Crystal chemistry, stoichiometry, and electrical and magnetic properties of phases of the $FeNb_3Se_{10}$ structure type

R. J. Cava, F. J. DiSalvo, M. Eibschutz, and J. V. Waszczak
Bell Laboratories, Murray Hill, New Jersey 07974
(Received 1 February 1983)

We have found the true stoichiometry of the phase first reported as $Fe_{0.25}Nb_{0.75}Se_{12}$, and later as $FeNb_3Se_{10}$, to be $Fe_{1+x}Nb_{3-x}Se_{10}$, with $0.25 \leq x \leq 0.40$. Compounds with the $FeNb_3Se_{10}$ structure type are relatively rare among transition-metal selenides. We report the synthesis and temperature-dependent magnetic susceptibility and resistivity of the new compounds $Fe_{1.33}Ta_{0.67}Nb_2Se_{10}$ and $Fe_{1-y}V_{1+y}Nb_2Se_{10}$, with $0.0 \leq y \leq 0.5$. The magnetic susceptibility and Mössbauer-effect measurements on $Fe_{1+x}Nb_{3-x}Se_{10}$ are dominated by the Fe-Nb disorder on the zigzag octahedral chains.

Transition-metal chalcogenides have been the subject of many studies with regard to phase transitions involving the formation of charge-density waves (CDW's). In $NbSe_3$ for example, two incommensurate CDW's have been observed, with onset temperatures of 144 and 59 K.[1,2] Recently, a new compound, nominally $FeNb_3Se_{10}$, with a crystal structure related to that of $NbSe_3$, has been reported.[3–5] The resistivity increases by 9 orders of magnitude as the temperature is lowered from 140 to 3 K. The onset of the resistivity rise occurs at approximately the same temperature as the formation of an incommensurate CDW.[3] The CDW onset temperature, 140 K, and periodicity, $q=(0.0,0.24,0.0)$, are only slightly different from those of the high-temperature CDW in $NbSe_3$ [144 K, $q=(0.0,0.27,0.0)$].

X-ray crystallographic studies[4,5] have shown the structure of $FeNb_3Se_{10}$ to consist of two $NbSe_6$ trigonal prismatic chains that have the same interatomic distances as one of the three types of trigonal prismatic chains in $NbSe_3$, and a double chain of edge shared $(Fe,Nb)Se_6$ octahedra, both running parallel to the monoclinic b axis. The chains are joined to form two-dimensional slabs separated by van der Waals gaps perpendicular to the chain direction. The structure of $FeNb_3Se_{10}$ is presented in Fig. 1. The Fe and Nb atoms on the octahedral chains, occurring in approximately a 1:1 ratio, are randomly distributed. The structural studies, finding metal atom disorder on the octahedral chains, further reinforced the interpretation[3] of the resistivity rise as in part being due to Anderson localization in the presence of a CDW.[6–8] It has been suggested[4] based on the structural similarities with $NbSe_3$, that the CDW in $FeNb_3Se_{10}$ occurs primarily on the $NbSe_6$ trigonal prismatic chains. The CDW on this chain would be effected by the disorder on the nearby Fe and Nb octahedral chains. Recent band-structure calculations of Whangbo *et al.*[9] also suggest that the electrons responsible for conduction and the CDW occur primarily in the prismatic chains.

The purpose of the present study is threefold. Firstly, since structural disorder has been shown to be present, a range of Fe and Nb populations might occur on the octahedral chains. To investigate that

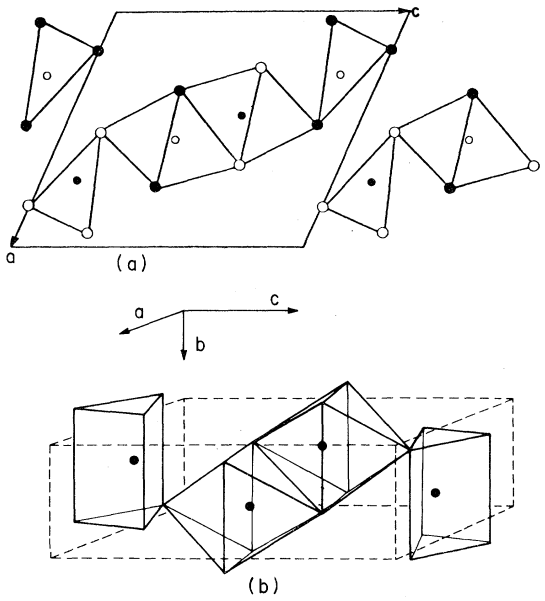

FIG. 1. (a) Projection of the $FeNb_3Se_{10}$ structure type along the monoclinic b axis shows the two trigonal prismatic and two octahedral chains per unit cell. The Se atoms are at the positions indicated by the larger circles (open circles at $z=0$, closed circles at $z=\frac{1}{2}$). (b) Projection of the $FeNb_3Se_{10}$ structure from a view almost perpendicular to the chains.

possibility, we have synthesized compounds of the type $Fe_{1+x}Nb_{3-x}Se_{10}$ and have found a small range of stoichiometries to occur, with $0.25 \leq x \leq 0.40$, but not at $x=0$ as was previously thought.[4-6] Secondly, we attempted to synthesize other compounds that could be expected to adopt this structure. One subset is of the type $M_{1+x}Nb_{3-x}Se_{10}$, where M prefers octahedral coordination with Se over trigonal prismatic coordination. A second subset is of the type $(M^1,M^2)_2Nb_2Se_{10}$, where we concentrated primarily on M^1=Fe and M^2= elements in columns IV*B*, V*B*, and VI*B*. In general, we have found the occurrence of the disordered $FeNb_3Se_{10}$-type phase to be extremely limited, with clear successes only for V and Ta substitution for the octahedral Nb. Finally, a phase of composition $M_2Nb_2Se_{10}$ of the $FeNb_3Se_{10}$ structure type would contain octahedral MSe_6 octahedral chains with no disorder and would be expected to show quite different electrical properties from those presently known. We have found no compounds of that type. We report in the following the extent of our synthetic experiments and the crystallographic, electrical, and magnetic properties of the $FeNb_3Se_{10}$-type compounds which we have found to exist.

SYNTHESIS AND CHARACTERIZATION

Powders of the appropriate compositions were synthesized from mixtures of the elements to study the chemistry of $FeNb_3Se_{10}$-type phases. They were mixed in batches of 4 to 5 g with each constituent weighed to an accuracy of ± 0.1 mg. Reactions were carried out in sealed evacuated quartz tubes at temperatures between 525–575 °C. After the initial reaction, the product was crushed, pressed into a pellet, and annealed. The crushing and pelletizing process was repeated until the powder x-ray diffraction patterns (Cu $K\alpha$ radiation) showed no change in two successive anneals. In each case, the final annealing temperature was taken as the maximum temperature to which the mixture could be heated without the formation of free selenium in the tube. The equilibrium phase assemblages were thus obtained, in periods of 1–2 weeks of annealing time. Compounds were considered to be single phase when no powder diffraction lines except those from the $FeNb_3Se_{10}$-type phase were present. The techniques employed allow us to observe the presence of crystalline impurity phases at about the 0.5% level, and thus the composition of a single phase product is exactly specified.

Resistivity measurements were performed on single crystal samples when they could be prepared by sublimation, as previously reported for $FeNb_3Se_{10}$ (Ref. 3-6), or by iodine vapor transport. In some cases single crystals of the proper phase could not be obtained by these techniques. Consequently, sintered powder compacts in the form of small rectangular bars were prepared by pressing single phase powder at 40 000 psi and heating in an evacuated quartz tube to 500 °C for 12 h.

RESULTS

The compositions investigated to determine the extent of occurrence of the $FeNb_3Se_{10}$-type phase are presented in Table I. The first entries (group A) characterize the range of Fe and Nb substitution in $Fe_{1+x}Nb_{3-x}Se_{10}$. The phase exists only for $0.25 \leq x \leq 0.40$ (not for $x=0$). For $x > 0.40$, the impurity phase was $FeSe_2$, and for $x < 0.25$ it was $NbSe_3$. The compositions have been synthesized for only an M_4Se_{10} stoichiometry. Compositions of the

TABLE I. Nominal compositions investigated to determine the extent of occurrence of the $FeNb_3Se_{10}$-type phase.

A. $Fe_{1+x}Nb_{3-x}Se_{10}$

$x = -0.50, -0.33, 0.0, 0.1, 0.2, 0.25, 0.33, 0.40, 0.50, 0.67$

B. $M_{1+x}Nb_{3-x}Se_{10}$

$FeNb_3Se_{10}$	$Fe_{1.33}Nb_{2.67}Se_{10}$
$NiNb_3Se_{10}$	$Ni_{1.33}Nb_{2.67}Se_{10}$
$CoNb_3Se_{10}$	$Co_{1.33}Nb_{2.67}Se_{10}$
$CrNb_3Se_{10}$	$Cr_{1.33}Nb_{2.67}Se_{10}$
$MnNb_3Se_{10}$	
$RuNb_3Se_{10}$	

C. $(M^1,M^2)^{oct}Nb_2^{TP}Se_{10}$

$FeTiNb_2Se_{10}$	$FeVNb_2Se_{10}$
$FeZrNb_2Se_{10}$	$FeTaNb_2Se_{10}$
$FeHfNb_2Se_{10}$	$FeMoNb_2Se_{10}$
$FeSnNb_2Se_{10}$	$CrTiNb_2Se_{10}$
$InSnNb_2Se_{10}$	$CrZrNb_2Se_{10}$

D. (Fe-V-Nb)Se_{10}

FeV_3Se_{10}	$Fe_{0.5}V_{1.5}Nb_2Se_{10}$
$FeNbV_2Se_{10}$	$Fe_{1.0}V_{1.0}Nb_2Se_{10}$
$Fe_{1.33}Nb_{0.67}V_2Se_{10}$	$Fe_{1.33}V_{0.67}Nb_2Se_{10}$
	$Fe_{1.5}V_{0.5}Nb_2Se_{10}$

E. (Fe-Ta-Nb)Se_{10}

$FeTa_3Se_{10}$	$FeTaNb_2Se_{10}$
$Fe_{1.33}Ta_{2.67}Se_{10}$	$Fe_{1.33}Ta_{0.67}Nb_2Se_{10}$
$FeNbTa_2Se_{10}$	

F. $M_2Nb_2Se_{10}$

$Al_2Nb_2Se_{10}$	$V_2Nb_2Se_{10}$
$Ga_2Nb_2Se_{10}$	$Cr_2Nb_2Se_{10}$
$In_2Nb_2Se_{10}$	$Fe_2Nb_2Se_{10}$
$Ti_2Nb_2Se_{10}$	
$Zr_2Nb_2Se_{10}$	

TABLE II. Monoclinic unit cells of phases of the $FeNb_2Se_{10}$ type.

Compound	a	b	c	β
$Fe_{1.25}Nb_{2.75}Se_{10}$	9.222(3)	3.478(1)	10.304(4)	114.55(3)
$Fe_{1.4}Nb_{2.6}Se_{10}$	9.223(4)	3.480(1)	10.310(3)	114.52(3)
$Fe_{0.5}V_{1.5}Nb_2Se_{10}$	9.216(2)	3.458(1)	10.221(3)	114.30(3)
$FeVNb_2Se_{10}$	9.230(2)	3.464(1)	10.206(3)	114.11(3)
$Fe_{1.33}Ta_{0.67}Nb_2Se_{10}$	9.223(3)	3.483(1)	10.338(2)	114.67(2)

type $Fe_yFe_{1.33}Nb_{2.67}Se_{10}$, $0.25<y<1.0$, were two phase, implying that intercalation of Fe cannot occur to a significant extent. The second (B) entries represent efforts to synthesize $FeNb_3Se_{10}$-type compounds with different transition metals substituted for Fe. Only for the Cr substitution, $CrNb_3Se_{10}$ and $Cr_{1.33}Nb_{2.67}Se_{10}$, was a compound of the $FeNb_3Se_{10}$ type observed. Neither of those compositions could be made single phase, however, and thus the exact chemical composition of the $FeNb_3Se_{10}$-type phase could not be determined. Of the entries (C) only $CrTiNb_2Se_{10}$ showed the existence of the $FeNb_3Se_{10}$-type compound, but the product was not single phase. Notable failures in entries (D) and (E), Table I, are that FeV_3Se_{10}, $FeTa_3Se_{10}$, and $Fe_{1.33}Ta_{2.67}Se_{10}$ do not form in the $FeNb_3Se_{10}$ structure type. We did, however, find that vanadium could be substitued for iron and niobium to a significant extent, in a phase of the type $Fe_{1-x}V_{1+x}Nb_2Se_{10}$, with $0.0\leq x\leq 0.50$. These are the only compounds that could be synthesized with fewer than 1 iron per formula unit. For the tantalum and niobium substitutions, only one substitution, $Fe_{1.33}Ta_{0.67}Nb_2Se_{10}$, was successful. Unlike the vanadium-based compounds, this compound showed no evidence for a range of solid solution. The final entries in Table I (F) describe efforts to obtain phases of stoichiometry $M_2Nb_2Se_{10}$, which would not display disorder on the octahedral chains. None of these compositions showed evidence for the oc-

TABLE III. Powder x-ray diffraction patterns for $FeNb_3Se_{10}$-type phases.

				$Fe_{1.25}Nb_{2.75}Se_{10}$		$Fe_{1.4}Nb_{2.6}Se_{10}$		$Fe_{0.5}V_{1.5}Nb_2Se_{10}$		$FeVNb_2Se_{10}$		$Fe_{1.33}Ta_{0.67}Nb_2Se_{10}$	
h	k	l	I/I_0	d_{obs}	d_{calc}	d_{obs}	d_{calc}	d_{obs}	d_{calc}	d_{obs}	d_{calc}	d_{obs}	d_{calc}
1	0	0	25	8.417	8.389	8.433	8.391	8.401	8.400	8.465	8.424	8.385	8.381
−1	0	1	10	8.161	8.158	8.184	8.159	8.094	8.117	8.154	8.110	8.177	8.175
1	0	1	35	5.262	5.258	5.268	5.262	5.252	5.255	5.277	5.268	5.258	5.258
−1	0	2	10	5.099	5.089	5.096	5.091	5.056	5.049	5.053	5.040	5.117	5.106
−2	0	1	5	4.604	4.608	4.611	4.609	4.596	4.604	4.611	4.610	4.608	4.609
−3	0	1						3.051	3.050	3.059	3.056		
−3	0	2	10	3.016	3.015	3.015	3.015	3.008	3.008	3.012	3.009	3.019	3.017
−2	1	1	100	2.774	2.776	2.776	2.777	2.762	2.765	2.768	2.769	2.777	2.779
−3	0	3	5	2.721	2.719	2.720	2.720	2.706	2.706	2.705	2.704	2.725	2.725
−2	1	2						2.630	2.632	2.634	2.634	2.628	2.629
1	0	3	15	2.597	2.596	2.599	2.598	2.587	2.587	2.592	2.590	2.599	2.599
−1	0	4	35	2.547	2.548	2.547	2.549	2.528	2.528	2.524	2.525	2.556	2.555
2	1	1	10	2.412	2.411	2.415	2.412	2.406	2.405	2.413	2.411	2.413	2.412
−2	1	3	5	2.365	2.366	2.370	2.367	2.351	2.351	2.353	2.351	2.373	2.372
0	0	4	5	2.345	2.343	2.347	2.345	2.328	2.329	2.328	2.329		
3	1	0	20	2.180	2.179	2.180	2.180	2.178	2.176	2.182	2.181	2.178	2.179
−3	1	3	10	2.143	2.142	2.143	2.143	2.132	2.131	2.131	2.131	2.146	2.146
4	0	0								2.104	2.106		
1	1	3	25	2.079	2.080	2.080	2.082	2.071	2.071	2.074	2.074	2.083	2.083
−1	1	4	20	2.053	2.055	2.054	2.056	2.042	2.041	2.040	2.040		
−3	0	5	5	1.985	1.984	1.985	1.985			1.966	1.966	1.990	1.991
2	1	3								1.808	1.808		
−5	0	1	10	1.784	1.785	1.784	1.785	1.787	1.787	1.791	1.791		
−5	0	4								1.744	1.745		
0	2	0	15	1.739	1.739	1.740	1.740	1.729	1.729	1.732	1.732	1.741	1.741
−3	1	5	5			1.724	1.724	1.713	1.711	1.709	1.710	1.728	1.728

currence of an $FeNb_3Se_{10}$-type compound (except for $Fe_2Nb_2Se_{10}$, which was not single phase).

Table II summarizes the phases of the $FeNb_3Se_{10}$ type found in this study. Included are the monoclinic lattice parameters for the compounds, as determined from least-squares fits to 20–25 clearly resolved lines observed in powder diffraction patterns below $2\theta=90°$ (Si powder internal standard). The lattice parameters for the end members of the $Fe_{1+x}Nb_{3-x}Se_{10}$ solid solution ($x=0.25$, $x=0.40$) are identical within the error of the measurement, and in good agreement with the parameters obtained previously for powders.[3] Partial substitution of vanadium for iron and niobium decreases all the cell parameters somewhat, as expected. Within the solid solution range of the compounds $Fe_{1-x}V_{1+x}Nb_2Se_{10}$, there are small but significant changes in the lattice parameters. The parameters determined for $Fe_{1.33}Ta_{0.67}Nb_2Se_{10}$ differ significantly from those of the $Fe_{1+x}Nb_{3-x}Se_{10}$ solid solution only for c and β. The observed and calculated d values for the lattice parameter fits are presented in Table III. Also included are the relative intensities of the powder diffraction lines for $Fe_{1.4}Nb_{2.6}Se_{10}$. The powder diffraction intensities for the other compounds are similar to those tabulated.

MAGNETIC SUSCEPTIBILITY, MÖSSBAUER SPECTRA, AND ELECTRICAL RESISTIVITY

The magnetic susceptibility of the powder samples was measured by the Faraday method from 4.2 to 600 K. The results for $Fe_{1+x}Nb_{3-x}Se_{10}$ at ($x=0.33$) shown in Fig. 2 are similar to those reported for single crystals whose composition was thought to be $FeNb_3Se_{10}$.[3] The data at $x=0.25$ and 0.40 are similar to those shown in Fig. 2, the susceptibilities of the three different compositions differ by no more than 10% above 10 K. The susceptibility is unusual in two ways: (1) At low temperatures a large Curie-Weiss contribution to the susceptibility is apparent. (2) The susceptibility is highly paramagnetic and above 200 K increases with increasing temperature.

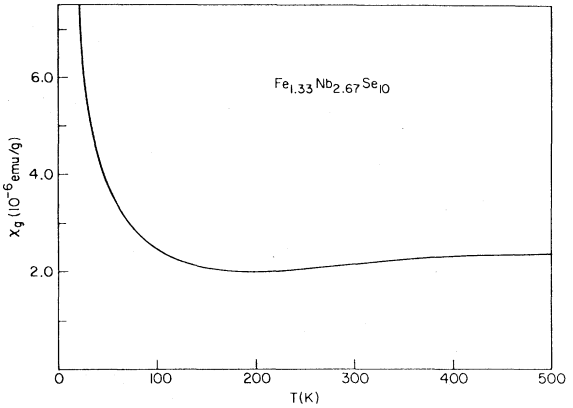

FIG. 2. Magnetic susceptibility of $Fe_{1.33}Nb_{2.67}Se_{10}$ shows a Curie contribution at low temperatures but then a minimum near 200 K.

The low-temperature susceptibility (<100 K) fits the usual Curie-Weiss expression $\chi_g=C_g/(T+\Theta)+\chi_0$ where C_g is the Curie constant, Θ the Weiss temperature, and χ_0 a temperature-independent term. A normalized least-squares fit[10] of the data below 100 K allows a determination of C_g, Θ, and χ_0 as given in Table IV for single-phase materials of this structure type. The goodness of fit ϵ is estimated by the rms fractional deviation of the data from the above form. Also included is the *average* effective moment per Fe obtained from the Curie constant. Since the susceptibility reaches a minimum near 200 K, it is apparent that the Curie-Weiss law is not an adequate description of the data above 100 K. A similar increase in susceptibility above 100 K is seen for all the samples listed in Table IV.

The Mössbauer spectrum of $Fe_{1.33}Nb_{2.67}Se_{10}$ powder (prepared with isotopically enriched ^{57}Fe) at 300 K is shown in Fig. 3. The data were fit with four independent Lorentzian lines, since four minima are seen in the spectrum, by a nonlinear least-squares method. The four Lorentzians obtained are also shown in Fig. 3, and their position, linewidth, and area are given in Table V. The linewidths are broader than those expected or observed in similar

TABLE IV. Curie-Weiss contribution to the magnetic susceptibilities of $FeNb_3Se_{10}$-type phases: $\chi_g=Cg(T+\Theta)+\chi_0$.

Compound	χ_0 (10^{-6} emu/g)	Cg (10^{-6} emu K/g)	Θ (K)	μ_{eff}/Fe at. (μ_B)	ϵ (%)	Temp. (K)
$Fe_{1.25}Nb_{2.75}Se_{10}$	1.05	135.0	2.5	0.93	0.23	10–100
$Fe_{1.33}Nb_{2.67}Se_{10}$	1.05	143.0	2.1	0.98	0.30	7–75
$Fe_{1.4}Nb_{2.6}Se_{10}$	1.08	146.0	2.0	0.96	0.36	7–75
$Fe_{1.33}Ta_{0.67}Nb_2Se_{10}$	1.08	152.0	2.5	1.14	0.37	10–100
$Fe_{0.5}V_{1.5}Nb_2Se_{10}$	0.49	103.0	3.0	1.34	0.57	4–100
$Fe_{1.0}V_{1.0}Nb_2Se_{10}$	0.45	128.0	3.8	1.05	0.23	9–75

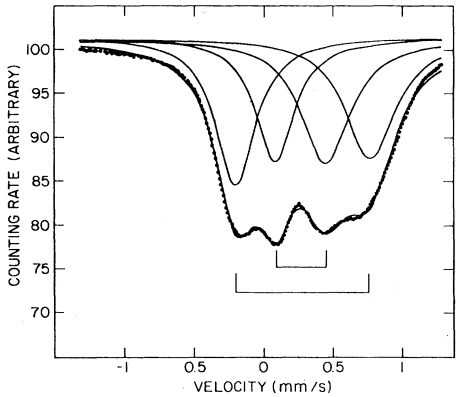

FIG. 3. Mössbauer spectrum of $Fe^{57}_{1.33}Nb_{2.67}Se_{10}$ at 300 K. The solid line shows the best fit of the spectrum to four independent Lorentzian lines.

compounds with the same sample absorbance (≈ 0.30 mm/sec). Since the areas of each line are approximately equal, we assume as a first approximation that this spectrum is due to two different Fe sites and represents two different quadrupole splittings. These two distinct sites could be produced by different near-neighbor cation distributions. For example, a particular cation in one of the octahedral chains has two nearest-neighbor cations—both in the adjacent octahedral chain.[4,5] If the distribution of Fe and Nb is totally random, then the probability of 2 Fe nearest neighbors to a particular Fe site is $\frac{4}{9}$, of one Fe nearest neighbor is $\frac{4}{9}$, and of no Fe nearest neighbors is $\frac{1}{9}$ (for $Fe_{1.33}Nb_{2.67}Se_{10}$). If the quadrupole splitting (QS) of the $\frac{1}{9}$ case is similar to one of the other two, or if the distribution of Fe and Nb atoms is not totally random so that only two possibilities occur with approximately equal probability (as might occur, for instance, if there were short-range Fe-Nb order on the octahedral chains), then a spectrum similar to that observed might be expected. That the nearest-neighbor cation distribution could have such a large effect on the QS seems plausible, since the cations in the adjacent octahedral chains are significantly displaced from the octahedra centers (on average) toward each other.[4,5] The excess line broadening and the small deviations of the data from the fit are assumed to be caused by the cation randomness on the octahedral chains beyond nearest neighbors. Fitting the data to a Gaussian distribution of Lorentzians does not affect the center of gravity of each peak. By using the center shifts obtained from the two Fe site fit, we can pair the peaks together to produce the simple quadrupole split spectra expected for each site. There are only three possible combinations of peaks (using numbers from Table V): (a) 1+2 and 3+4, (b) 1 + 3 and 2 + 4, or (c) 1 + 4 and 2 + 3. The center shifts for each of these cases are (a) 0.13 and 0.87 mm/sec, (b) 0.33, and 0.66 mm/sec, and (c) 0.51 and 0.49 mm/sec, respectively. At 4.2 K the Mössbauer-effect spectrum (Fig. 4) shows only two broad resonance lines with a center shift of 0.57 mm/sec. The collapse of two quadrupole peaks into only one quadrupole is consistent with the existence of an incommensurate CDW at low temperature.[11,12] The 4.2 K center shift result indicates that combination *c* is correct, and that Fe is in the same valence state as a function of temperature. The quadrupole splitting is temperature dependent. The room-temperature values for the quadrupole splittings from model *c* are 1.08 and 0.41 mm/sec and at 4.2 K 0.76 mm/sec.

TABLE V. Room-temperature values for Mössbauer peak positions, full width at half maximum (FWHM) and area for $Fe^{57}_{1.33}Nb_{2.67}Se_{10}$.

Line	Position[a] (mm/sec)	FWHM (mm/sec)	Area (arb. units)
1	−0.034	0.40	9.03
2	0.285	0.39	7.47
3	0.690	0.48	9.55
4	1.048	0.48	9.30

[a]With respect to iron metal.

Resistivity measurements using the standard four-probe technique were performed on samples with the compositions shown in Table IV. Single crystals could be obtained by sublimation from powders of $Fe_{1+x}Nb_{3-x}Se_{10}$, but x-ray fluorescence indicated that the composition of these crystals was independent of the stoichiometry of the powder composition ($0.25 < x < 0.40$). These crystals are in the form of long needles that grow parallel to the chain direction. The resistivity measured along the chains is identical to that previously reported.[3,5]

Needlelike crystals grown by iodine transport

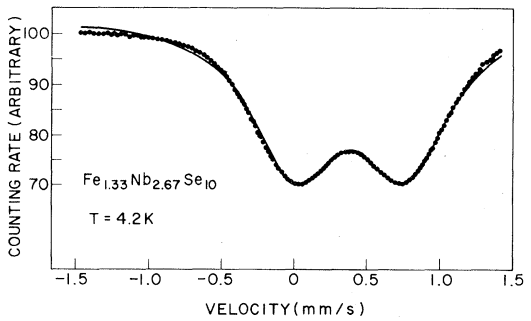

FIG. 4. Mössbauer spectrum of $Fe^{57}_{1.33}Nb_{2.67}Se_{10}$ at 4.2 K. The solid line shows the best fit of the spectrum of two independent Lorentzian lines.

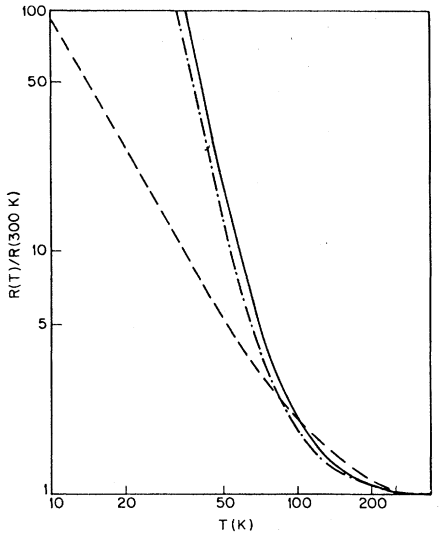

FIG. 5. Electrical resistance of several crystals parallel to the needle axis shows the large increase at low temperatures. The solid line is obtained from a crystal sublimed from $Fe_{1.33}Nb_{2.67}Se_{10}$, the dashed-dotted line from the same composition but grown by iodine vapor transport, and the dashed line from a crystal grown by iodine vapor transport from a two-phase powder of nominal composition $FeTaNb_2Se_{10}$.

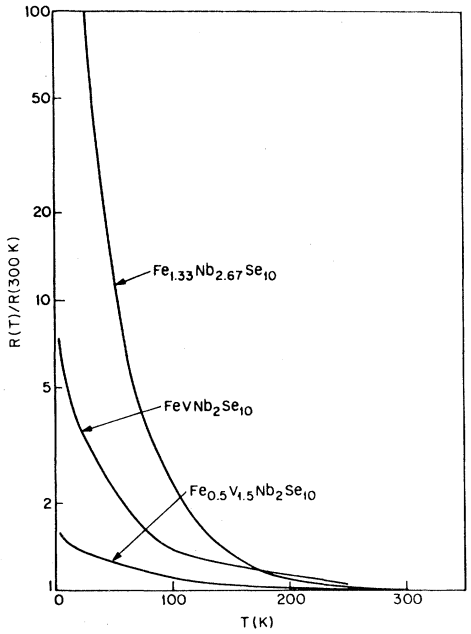

FIG. 6. Electrical resistivity of sintered pellets of powders of the indicated composition shows a low-temperature increase that increases with Fe content.

from a multiphase powder of nominal composition $FeTaNb_2Se_{10}$ have the same structure as the single phase $Fe_{1.33}Ta_{0.67}Nb_2Se_{10}$ powder and x-ray fluorescence shows that the Ta content of the crystals and single phase powder is similar. The resistivity of these crystals is compared to that of the nominal $FeNb_3Se_{10}$ crystals in Fig. 5. It is apparent that the resistivity rise in the Ta-containing crystals is much less at low temperatures than that of the samples containing only Nb.

Crystals of $Fe_{1-x}V_{1+x}Nb_2Se_{10}$ could not be prepared, thus the resistivity was obtained on pressed and sintered powder compacts. The conductivity of compounds having the $FeNb_3Se_{10}$ structure type is expected to be quite anisotropic, but this anisotropy has not been measured. Consequently, we measured the resistivity of a sintered pellet of $Fe_{1.33}Nb_{2.67}Se_{10}$ for comparison. The results are shown in Fig. 6.

DISCUSSION

One of the striking aspects of this new "$FeNb_3Se_{10}$"-type phase is the limited extent to which it forms. At present we have found no sulfide analogs, and have found that Fe can only be substituted to a large extent by Cr. The Nb in the octahedral site can be replaced only by V or Ta; however, the fully substituted analogs $Fe_{1+x}M_{3-x}Se_{10}$ with $M=$V or Ta do not exist. Apparently this new structure is only slightly more stable than the related binary phases: the di- and trichalcogenides of the respective transition metals. Although we confirm the reported existence[13] of a Cr-containing M_4Se_{10} phase of this type, we do not confirm its reported stoichiometry $Cr_2Nb_2Se_{10}$. In addition, the reported[13] vanadium-containing phase $FeVNb_2Se_{10}$ is found to have a stoichiometry range between $Fe_{0.5}V_{1.5}Nb_2Se_{10}$ and $FeVNb_2Se_{10}$ when synthesized between 525–575 °C.

The magnitude of the *average* Fe magnetic moments (Table IV) is low for Fe^{3+} or Fe^{2+} high spin and Fe^{3+} low spin, and cannot be due to Fe^{2+} low spin. The Mössbauer isomer shift of about 0.57 mm/sec is on the low end of the range expected for Fe^{2+} high spin and the high end of the Fe^{3+} high-spin range,[11,14] but the magnetic susceptibility data are consistent with a high-spin assignment, if there are large exchange interactions between the Fe atoms in adjoining octahedral sites. The exchange pathways as seen from Fig. 1 form one-dimensional ladders. This is consistent with the magnetic susceptibility results over the whole temperature range.

The important aspects of our interpretation of the magnetic data are as follows. We consider only two antiferromagnetic exchange interactions: (1) between Fe atoms that are near neighbors on the same octahedral chain, and (2) between two Fe atoms that are near neighbors on adjoining octahedral chains.

All other interactions are assumed weak. The strong exchange interactions exist only on each ladder (double octahedral chain, one per unit cell), but not between ladders (different unit cells). Unless the Fe and Nb are completely ordered on the octahedral chains (which they are not) clusters of Fe atoms will form. Some of these clusters will have one-dimensional exchange pathways, while others will contain triangular loops. Depending upon the nature (e.g., Heinsenberg or Ising) and magnitude of the exchange interactions at least some of the clusters will have a net magnetic moment that will be less than the moment on each individual Fe (at temperatures lower than the antiferromagnetic exchange temperature). Such clusters are likely to contain an odd number of Fe atoms. Since many of the clusters can be approximated as one-dimensional chains, their magnetic properties should be similar to those calculated for one-dimensional chains by Bonner and Fischer.[15] Indeed, the temperature dependence of the measured susceptibility shown in Fig. 2 is very similar to the calculated susceptibility of odd number chains. Qualitatively we expect that the magnetic susceptibility of such a collection of clusters to be equal to $N_0 g^2 S(S+1)\mu_B^2/3k(T+T_0)$ [Eq. (1)] for $T \gg T_0$, where N_0 is the number of Fe atoms and T_0 is determined by the exchange interaction J. As the temperature is lowered, the susceptibility goes through a maximum $X_{\max}$ near T_0 at a value of susceptibility about a factor of 2 lower than that given by Eq. (1). At low temperatures the susceptibility will be approximately $Ng^2S(S+1)\mu_B^2/3k(T+\Theta)+X_0$, where N is the number of clusters with an uncompensated spin, Θ is determined by *intercluster* exchange, and X_0 is the Van Vleck susceptibility of the antiferromagnetically coupled spins (typically $X_0 \approx X_{\max}/2$).

This qualitative model indeed seems to explain the observed results if we assume $T_0 \approx 500$ K and $N \approx 0.04 N_0$ and an iron moment of approximately $5\mu_B$ for $Fe_{1.33}Nb_{2.67}Se_{10}$. The magnitude of the susceptibility at $T=500$ K calculated from Eq. (1) is about 3×10^{-6} emu/g, somewhat higher than that measured, as expected.

Other sources of paramagnetism are unlikely to explain the large values observed above room temperature. $NbSe_3$ is diamagnetic; the susceptibility at 300 K is -0.21×10^{-6} emu/g.[16] The susceptibility of a high density-of-states chalcogenide compound $NbSe_2$ ($+0.76\times10^{-6}$ emu/g at 300 K) (Ref. 16) is also less than that of $Fe_{1.33}Nb_{2.67}Se_{10}$. Since the *d*-band widths calculated for $NbSe_3$ (Ref. 17) and $FeNb_3Se_{10}$ (Ref. 9) are very similar, it is unlikely that the large susceptibilities seen here are due to Pauli or Van Vleck paramagnetism of the conduction band.

At present, a detailed theoretical understanding of random antiferromagnetically coupled chains is not available. Consequently, we cannot fit detailed equations which could help us in determining the exact moment on each Fe atom.

The resistivity measurements in Figs. 5 and 6 all indicate a rise at low temperatures that is specific to the particular composition. In particular the data of Fig. 6 suggest that lower Fe concentrations produce weaker localization, a result not unexpected in an Anderson-type localization model. Unfortunately, no composition with low enough Fe concentration (or complete order on the octahedral sites such as in $M_2Nb_2Se_{10}$) to exhibit metalliclike low-temperature behavior was found.

SUMMARY

Few compounds having the $FeNb_3Se_{10}$ structure type were found to exist in our synthetic survey. These few compounds had similar magnetic susceptibilities: a Curie contribution at low temperatures, a minimum near 200 K, which rises to a broad maximum above 300 K at about 2×10^{-6} emu/g. The ^{57}Fe Mössbauer effect is dominated by the fact that Fe and Nb are randomly distributed in the octahedral chains, and is influenced by the incommensurate CDW on the trigonal prismatic chains. Finally, the low-temperature resistivity rise is seen to increase with increasing Fe concentration in these compounds. All the data remain consistent with the suggestions that a CDW occurs on the trigonal prismatic chains and that the CDW is influenced by the randomness in the cation found on the octahedral sites.

[1] P. Moneeau, N. P. Ong, A. M. Portis, M. Meerschaut, and J. Rouxel, Phys. Rev. Lett. 37, 602 (1976).
[2] R. M. Fleming, D. E. Moncton, and D. B. McWhan, Phys. Rev. B 18, 5560 (1978).
[3] S. J. Hillenius, R. V. Coleman, R. M. Fleming, and R. J. Cava, Phys. Rev. B 23, 1567 (1981).
[4] R. J. Cava, V. L. Himes, A. D. Mighell, and R. S. Roth, Phys. Rev. B 24, 3634 (1981).
[5] A. M. Meerschaut, P. Gressier, L. Greemas, and J. Rouxel, Mater. Res. Bull. 16, 1035 (1981).
[6] S. J. Hillenius and R. V. Coleman, Phys. Rev. B 25, 2191 (1982).
[7] N. Mott, M. Pepper, S. Pollitt, R. H. Wallis, and C. J. Adkins, Proc. R. Soc. London Ser. A 354, 169 (1975).
[8] F. J. DiSalvo, J. A. Wilson, and J. V. Waszczak, Phys. Rev. Lett. 36, 885 (1976).

[9]M. H. Whangbo, R. J. Cava, R. J. DiSalvo, and R. M. Fleming, Solid State Commun. 43, 277 (1982).
[10]F. J. DiSalvo, J. V. Waszczak, and M. Eibschutz, Phys. Rev. B 24, 5143 (1981).
[11]M. Eibschütz and F. J. DiSalvo, Phys. Rev. Lett. 36, 104 (1976).
[12]M. Eibschütz and F. J. DiSalvo, Phys. Rev. B 15, 5181 (1977).
[13]A. Ben Salem, A. Meerschaut, L. Guemas, and J. Rouxel, Mater. Res. Bull. 17, 1071 (1982).
[14]M. Eibschütz, Adv. Chem. Ser. 194, 523 (1981).
[15]J. Bonner and M. E. Fischer, Phys. Rev. 135, A640 (1964).
[16]F. J. DiSalvo, J. V. Waszczak, and K. Yamaya, J. Phys. Chem. Solids 41, 1311 (1980).
[17]R. Hoffmann, S. Shaik, J. C. Scott, M.-H. Whangbo, and M. J. Foshee, J. Solid State Chem. 34, 263 (1980).